THE ASTROPHYSICAL JOURNAL SUPPLEMENT SERIES, 73:159–163, 1990 June

NONPOTENTIAL MAGNETIC FIELDS AT SITES OF GAMMA-RAY FLARES

M. J. HAGYARD
Space Science Laboratory, Marshall Space Flight Center
P. VENKATAKRISHNAN
Indian Institute of Astrophysics
AND
J. B. SMITH, JR.
University of Alabama in Huntsville
Received 1988 December 9; accepted 1989 February 22

ABSTRACT

In this paper the relation between the degree of nonpotentiality of photospheric magnetic fields and the occurrence of gamma-ray flares is examined. We use the parameter $\Delta\Phi$ (termed magnetic "shear") and the strength of the magnetic field intensity as measures of the degree of nonpotentiality, where $\Delta\Phi$ is defined as the angular difference between the observed direction of the transverse component of the photospheric field and the direction of the potential field prescribed by the distribution of measured photospheric flux. An analysis of the great flare of 1984 April 24–25 is presented as an example of this technique to quantify the nonpotential characteristics of the preflare magnetic field. For this flare, which produced a large gamma-ray event, we found that strong shear and high field strengths prevailed over an extended length of the magnetic neutral line where the flare occurred. Moreover, the flare began near the area of strongest measured shear (89°–90°). Four other flaring regions were analyzed; one of these produced a moderate gamma-ray event while the other three did not produce detectable gamma rays. For all four regions the flares were located in the area where the local field was most nonpotential, regardless of the class of flare. The fields of the gamma-ray flares were compared with those associated with the flares without gamma rays, and we found little distinction in the degree of magnetic shear. The major difference is seen in the extent of the sheared field: for gamma-ray events, the field is sheared over a longer length of the neutral line.

Subject headings: gamma rays: general — hydromagnetics — radiation mechanisms — Sun: flares

I. INTRODUCTION

The source of energy of all flares is assumed to be the free energy stored in nonpotential magnetic fields concentrated along and near the magnetic "neutral line" separating fields of opposite polarity in solar active regions. With the advent of measurements of the transverse component of the Sun's photospheric magnetic field with instruments such as the Marshall Space Flight Center's vector magnetograph (Hagyard *et al.* 1982; Hagyard, Cumings, and West 1985), quantitative evaluations of the nonpotential nature of these fields can now be made. The line-of-sight component of the photospheric field can determine the structure of the potential field appropriate to that particular distribution of magnetic flux. This potential field can then be compared with the observed transverse field to determine where the field has been stressed into nonpotential configurations. Using this quantitative technique, we have analyzed MSFC observations of a number of flares observed during the last solar maximum period. Collectively, these analyses have shown that the magnetic field at the sites of ribbon flares is strongly nonpotential, and there is a statistical correlation between increased magnetic stress and increased flare activity (Hagyard *et al.* 1984, 1986).

In this paper we use a similar analysis to investigate the nonpotential characteristics of gamma-ray flares and determine whether there are special signatures of these stressed fields for this special class of flares. We present the results of an analysis of the active region of 1984 April, AR 4474, which produced one of the most intense flares of the last solar cycle on April 24. This study showed that the big flare initiated at the location on the magnetic neutral line where the field deviated the most from a potential field. We then compare the nonpotential signatures of AR 4474 with those of four other regions, one which produced a gamma-ray event and three which did not. Our tentative conclusion from this small data sample is that gamma-ray flares are associated with strongly nonpotential fields which extend over relatively larger lengths of the magnetic neutral line than the fields associated with flares producing no gamma-ray events.

II. ANALYSIS OF THE MAGNETIC FIELD OF ACTIVE REGION AR 4474

The active region, designated AR 4474 by NOAA, rotated onto the solar disk on 1984 April 22. The great flare erupted on April 24 at 23:57 UT and attained its maximum phase at 23:59 UT (Kurokawa *et al.* 1987). White-light brightenings appeared 4 minutes after the onset of the flare (Hiei, Zirin, and Wang 1986) which was classified as a 3B/X13 event and was one of the most intense flares observed by the *Solar Maximum Mission* (*SMM*) Gamma Ray Spectrometer.

Observations of the photospheric magnetic field of this active region were carried out with the MSFC vector magnetograph starting on April 24 at 22:11 UT; the last set of data was obtained near sunset, at 22:36 UT, 80 minutes prior to the onset of the great flare. The overall configuration of the line-of-sight component $B_{\|}$ of the magnetic field of AR 4474 at 22:11 UT is shown in Figure 1 (Plate 2) along with white-light and Hα images taken early and late on April 24 and again early on April 25 at the Hida Observatory (Kurokawa *et al.* 1987). Figure 2 (Plate 3) shows the development of the flare along the western part of the magnetic neutral line outlined in Figure 1 on the map of $B_{\|}$. In Figure 3*b* (Plate 4) the transverse component $B_{\perp}$ of the magnetic field in the area of the flare is shown superposed on the $B_{\|}$ field. In Figure 3*c* the potential field determined by $B_{\|}$ is displayed in a similar format. Comparison of the observed (Fig. 3*b*) and potential (Fig. 3*c*) fields along that portion of the neutral line bracketed by the flare ribbons seen in Figure 3*a* demonstrates that the observed field is highly nonpotential there.

This alignment of the transverse field more nearly parallel to the neutral line rather than perpendicular as in the case of the potential field leads to the terminology of magnetic "shear." Studies of the proper motions of the spots in this region by Kurokawa *et al.* (1987) and Gesztelyi and Kalman (1986) clearly indicate that the sheared configuration of the transverse field connecting the opposite polarities across the western section of the magnetic neutral line was probably formed in response to the westward motion of the negative-polarity sunspot located in the lower right part of Figure 3*a*.

With the data shown in Figures 3*b* and 3*c*, we can characterize the magnetic shear in a quantitative way by calculating the parameter $\Delta\Phi$, defined as the difference between the observed direction of the transverse field and the direction of the transverse potential field. If the field is nearly potential, then $\Delta\Phi \approx 0°$; for a highly sheared field, $\Delta\Phi \approx 90°$. In the analysis scheme, we identify the string of points forming the neutral line and calculate $\Delta\Phi$ at those points where the transverse field strength is above 200 G. To display the results we use the following criteria to select ranges of shear:

$$B_T \geq \frac{1}{2} B_T^{\max} \quad \text{and} \quad 70° \leq \Delta\Phi < 80°,$$

$$B_T \geq \frac{1}{2} B_T^{\max} \quad \text{and} \quad \Delta\Phi \geq 80°,$$

where $B_T^{\max}$ is the maximum field intensity along the relevant portion of the neutral line.

Figure 3*d* is a magnetic shear map of the data obtained at 22:36 UT. The dots indicate neutral-line points where $B_T >$ 200 G, the open circles indicate points consistent with the first criterion, and the filled squares indicate those consistent with the second one.

To allay concerns that projection effects might render these analyses invalid since the region was at a longitude offset of $-45°$, we carried out the same calculations after transforming the magnetic field components from the image-plane frame of reference to heliographic coordinates (Venkatakrishnan, Hagyard, and Hathaway 1988). The results obtained (Venkatakrishnan, Hagyard, and Hathaway 1989) showed only a minor change: one less circle and one less square in the heliographic coordinate system.

An earlier magnetogram, taken at 22:11 UT, was analyzed and compared with the later one to look for indications of an evolution of the shear; the resulting shear map is shown in Figure 4. In Table 1 the numerical values for B_T and $\Delta\Phi$ are given for the 15 points that correspond to the 15 circles and squares seen in Figures 3*d* and 4 along the western neutral line, starting with the northern three consecutive circles.

Comparing Figures 3*d* and 4 and looking at the numerical data given in Table 1, there does not seem to be any *overall* trend of a general increase or decrease in field strength or shear. All but two of the changes in field strength lie below the calculated noise level of 135 G for B_T and are therefore not significant. In the case of the shear parameter $\Delta\Phi$, the uncertainty in Φ was calculated to be $\approx 1°$–$2°$ for field strengths on the order of 1000 G. Thus we might take changes of 4° or more as significant if they occur at two or more consecutive pixels. Using this criterion, there is an indication of a decrease in shear at points 6 and 7, an increase at points 10 and 11, and an increase at points 14 and 15. To feel comfortable with designating these changes as truly significant, we would find it more reassuring if more than two consecutive points were involved. A conservative conclusion is that there is no extended region of increasing or decreasing shear.

Kurokawa *et al.* (1987) indicate that the first Hα brightenings of the flare were near the filament in the region of the

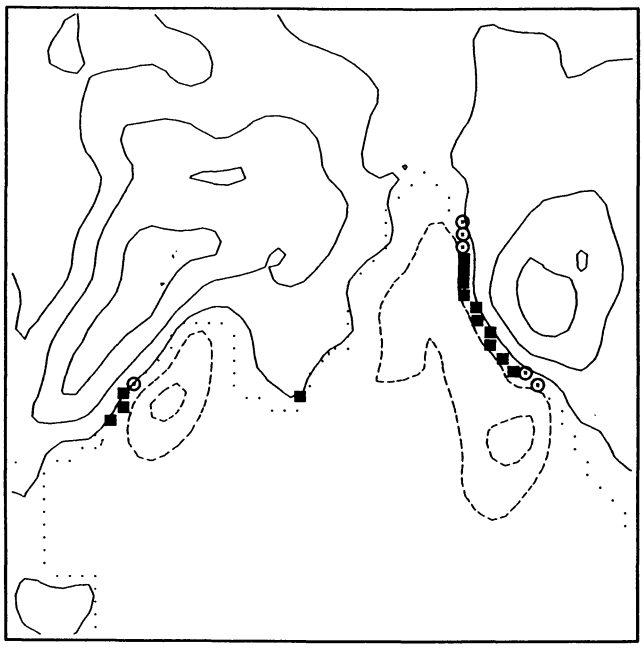

FIG. 4.—Persistence of high shear at the flare site on April 24. This map is similar in format to that of Fig. 3*d* but was derived from a vector magnetogram taken 25 minutes earlier.

TABLE 1

MAGNETIC INTENSITY AND SHEAR AT POINTS ALONG THE WESTERN NEUTRAL LINE

POINT	DATA AT 22:11 UT		DATA AT 22:36 UT	
	B_T(G)	$\Delta\Phi$	B_T(G)	$\Delta\Phi$
1	1225	73°	1315	70°
2	1325	73	1380	72
3	1320	77	1355	79
4	1235	83	1255	89
5	1110	89	1140	89
6	1095	89	1155	80
7	1180	90	1230	82
8	1360	84	1370	84
9	1360	81	1415	79
10	1590	82	1550	86
11	1715	82	1640	90
12	1725	87	1555	86
13	1420	83	1335	79
14	1360	77	1240	86
15	1055	75	980	84

neutral line to the north of the large negative spot and east of the positive spot seen Figures 3*d* and 4. This seems to place the location of flare onset near points 4–7 of Table 1. The flare then spread along the neutral line between the two sunspots. Thus the flare began near points having the strongest measured shear (89°–90°) prior to the flare and enveloped the whole area of strong shear and high field strength shown in Figures 3*d* and 4.

Magnetograph observations were obtained on April 25 at 16:25 UT, but instrumental problems that occurred have made it difficult to properly analyze the data for the postflare configuration of the photospheric field. Thus we cannot say at this time whether there was a change in the degree of nonpotentiality as a result of the large flare.

This same region produced a number of flares over the next 5 days, including a dozen M-class X-ray events and four flares classed as 2B. One of these latter occurred on April 28 at 20:17 UT. This particular flare, a 2B/C6 event, was located in the *eastern* portion of AR 4474, in the other area of significant shear seen in Figures 3*d* and 4. We analyzed a magnetogram taken at 19:53 UT, 24 minutes before the flare started; the shear map for this magnetogram is shown in Figure 5. There are two noteworthy points to be made about the areas of shear seen in this map. First, the large area of shear in the western spots—the region of the gamma-ray event on April 24—has persisted and indicates that this area is more nonpotential than the eastern region. However, in the time interval of 20:00 UT $\pm$ 4 hr, only subflares were observed there. This observation supports the idea that large shear alone is not a sufficient condition for major flares. The second point is that the shear in the eastern area on April 28 has increased from the values calculated on April 24; this increase can be seen by comparing Figures 3*d* and 4 with Figure 5. Remembering that large shearing motions occurred in the *western* area in the period April 23–24 before the gamma-ray flare and noting that an increase in shear took place between April 24–28 in the eastern area before the flare there, we conclude that increases in the length of the critically sheared region over a time scale of a few days could herald the onset of major flares.

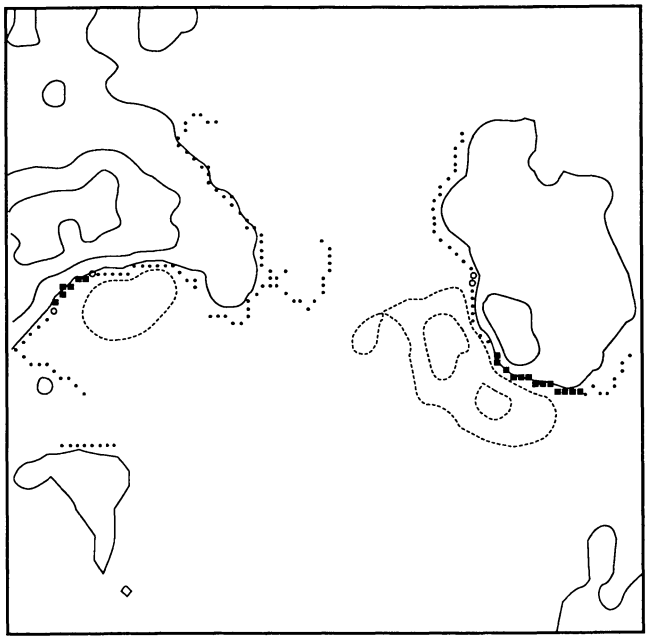

FIG. 5.—Magnetic shear along the neutral line of AR 4474 on April 28. This map was derived from a vector magnetogram obtained 24 minutes before the 2B/C6 flare at 20:17 UT. The field of view is 230″ × 230″, and west is to the right on the figure.

The flare on April 28 was not a gamma-ray event although it was a large flare by most standards. In comparing the nonpotential characteristics of the two areas of AR 4474, the significant difference between the area of the gamma-ray flare and the other highly sheared region is the length of the neutral line involved. In the next section we will investigate

whether this criterion holds for other active regions that we have analyzed.

III. ANALYSIS OF SHEAR FOR OTHER CLASSES OF FLARES

Similar analyses have been carried out for three other active regions of the last solar cycle; each of these regions produced a series of major flares. The first region, designated AR 4711, produced a major flare—3B/X3—and a gamma-ray event on 1986 February 4 at 07:41 UT. The preflare magnetic field was measured with the MSFC magnetograph at 16:42 UT on February 3; the image-plane map of the shear parameter $\Delta\Phi$ is shown in Figure 6. The flare occurred on that part of the neutral line where the nine solid squares and one open circle are located. Moreover, the initial flare brightenings were located in the area where there was a local maximum of angular shear.

In Figure 7 the shear map for AR 2776 at 14:23 UT on 1980 November 5 is shown. This data set preceded a 1B/M2 flare at 16:03 UT, the first major flare produced in this active region. The location of this flare again coincides with the area where the local field was the most nonpotential, i.e., where there was a coincidence of large shear and strong fields as indicated by the seven solid squares and one open circle. Here, too, the initial flare kernels were seen to bracket the neutral line where $\Delta\Phi$ was largest.

The last region, AR 2372, which was on the solar disk in 1980 April, produced a number of M-class flares and one X-class event in the period April 5–8. The magnetic data

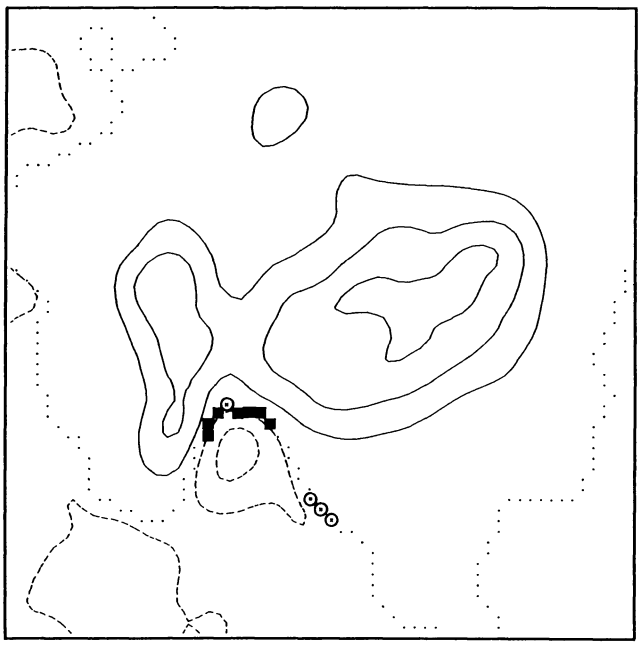

14:23 UT NOVEMBER 5, 1980

FIG. 7.—Magnetic shear map for AR 2776. The first major flare from this region, a 1B/M2 event at 16:03 UT on November 5, was located where this map indicates the highest shear existed. The field of view is 140″×140″, and west is to the right.

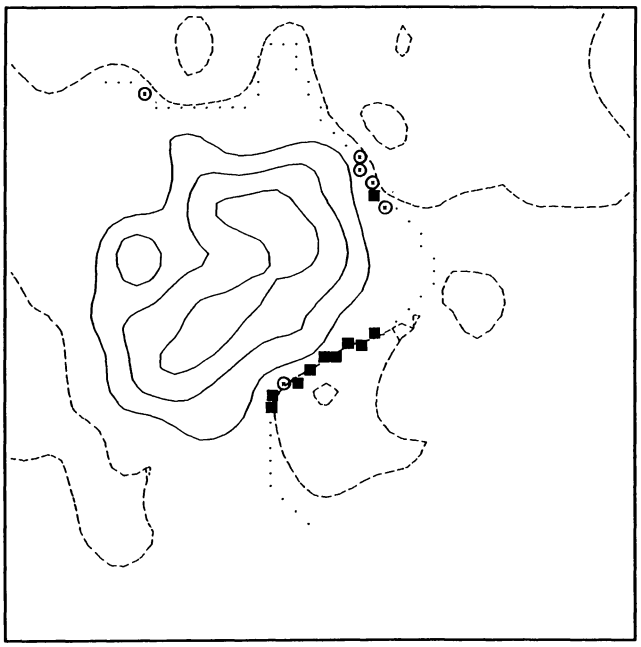

16:42 UT FEBRUARY 3, 1986

FIG. 6.—Magnetic shear map for AR 4711. This shear map was derived from a vector magnetogram obtained several hours prior to a 3B/X3 flare. The flare was centered along that portion of the neutral line where the shear was concentrated, as indicated by the solid squares. The field of view is 135″×135″, and west is to the left of the image.

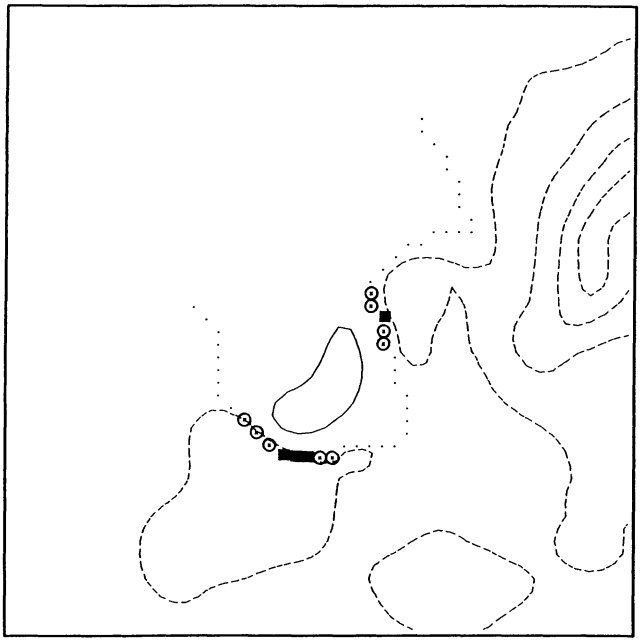

21:10 UT APRIL 6, 1980

FIG. 8.—Magnetic shear map for AR 2372. Flare ribbons of the 1B/M4 flare which occurred several hours after the magnetic field observations were made were located at both sites of high shear seen in this map. However, the flare onset was located in the area of the more extended length of shear. The field of view is 125″×125″, and west is down.

TABLE 2

COMPARISON OF NONPOTENTIALITY PARAMETERS FOR DIFFERENT FLARES

Date of Flare (1)	Max B_T(G) (2)	Max $\Delta\Phi$ (3)	Number of Points (4)	Flare Class (5)	γ Event (6)
1984 Apr 24 ...	1700	90°	15	3B/X13	yes
1984 Apr 28 ...	1920	90	8	2B/C6	no
1986 Feb 4	1100	90	10	3B/X3	yes
1980 Nov 5	1000	88	8	1B/M2	no
1980 Apr 7	1000	85	8	1B/M4	no

that were analyzed for shear were obtained in the middle of this period at 21:10 UT on April 6. The next major flare following the magnetic observations was a 1B/M4 event at 00:48 UT on April 7. The shear map for the observations at 21:10 UT is displayed in Figure 8. There are two areas of strong shear as defined by our criteria, and both were locations of flare ribbons. However, the flare onset was observed at the area of three solid squares and five open circles, and this is where the field intensity was highest and the shear strongest.

The results of these analyses are summarized in Table 2, where we have indicated for each flare the maximum observed transverse field strength on the relevant section of the magnetic neutral line (col. [2]), the maximum shear along that neutral line (col. [3]), the maximum number of *consecutive* points designated by open circles and filled squares (col. [4]), the flare class, (col. [5]), and whether there was a gamma-ray event detected (col. [6]).

IV. SUMMARY AND CONCLUSIONS

The results of this study indicate that for all four active regions studied, the five flares were located in an area where the local magnetic field deviated the most from a potential field, regardless of the class of flare. In addition, flare onset appears to occur preferentially at the point of greatest shear $\Delta\Phi$ along the relevant segment of the magnetic neutral line. However, there does not seem to be any distinctive difference in the degree of shear between flares that produce gamma-ray events and those that do not. A similar inference seems to pertain to the strength of the field. There does seem to be an indication that the gamma-event flares occur where strongly nonpotential fields extend over a relatively large area. This conclusion is based on the result that the number of consecutive points of high shear and strong fields is larger for the two gamma-ray flares of 1984 April 24 and 1986 February. Obviously, many more cases need to be analyzed before we can make a definitive statement as to the existence of any special signatures of gamma-ray flares that are seen in the magnetic field.

This work was done while one of us (P. V.) held a National Research Council–National Academy of Science Research Associateship. The observational programs that produced the magnetic data reported in this paper were carried out as part of the *SMM* Guest Investigator Program. Support for this research was provided by NASA through its Solar Physics Branch of the Space Physics Division and by the Air Force Geophysics Laboratory through its Solar Research Branch of the Space Physics Division.

REFERENCES

Gesztelyi, L., and Kalman, B. 1986, *Adv. Space Res.*, Vol. **6**, (6), 21.
Hagyard, M. J., Cumings, N. P., and West, E. A. 1985, in *Proc. Kunming Workshop on Solar Physics and Interplanetary Traveling Phenomena*, ed. C. De Jager and Chen Biao (Beijing: Science Press), p. 204.
Hagyard, M. J., Cumings, N. P., West, E. A., and Smith, J. E. 1982, *Solar Phys.*, **80**, 33.
Hagyard, M. J., Smith, J. B., Jr., Teuber, D., and West, E. A. 1984, *Solar Phys.*, **91**, 115.
Hagyard, M. J., *et al.* 1986, in *Energetic Phenomena on the Sun*, ed. M. R. Kundu and B. E. Woodgate (NASA CP-2439), p. 1.
Hiei, E., Zirin, H., and Wang, J. 1986, in *The Lower Atmosphere of Solar Flares*, ed. D. F. Neidig (Sunspot, NM: National Solar Observatory), p. 129.
Kurokawa, H., Hanaoka, Y., Shibata, K., and Uchida, Y. 1987, *Solar Phys.*, **108**, 251.
Venkatakrishnan, P., Hagyard, M. J., and Hathaway, D. H. 1988, *Solar Phys.*, **115**, 125.
_____. 1989, *Solar Phys.*, **122**, 215.

M. J. HAGYARD and J. B. SMITH, JR.: Space Science Laboratory, ES 52, Marshall Space Flight Center, AL 35812

P. VENKATAKRISHNAN: Indian Institute of Astrophysics, Bangalore 560034, India

PLATE 2

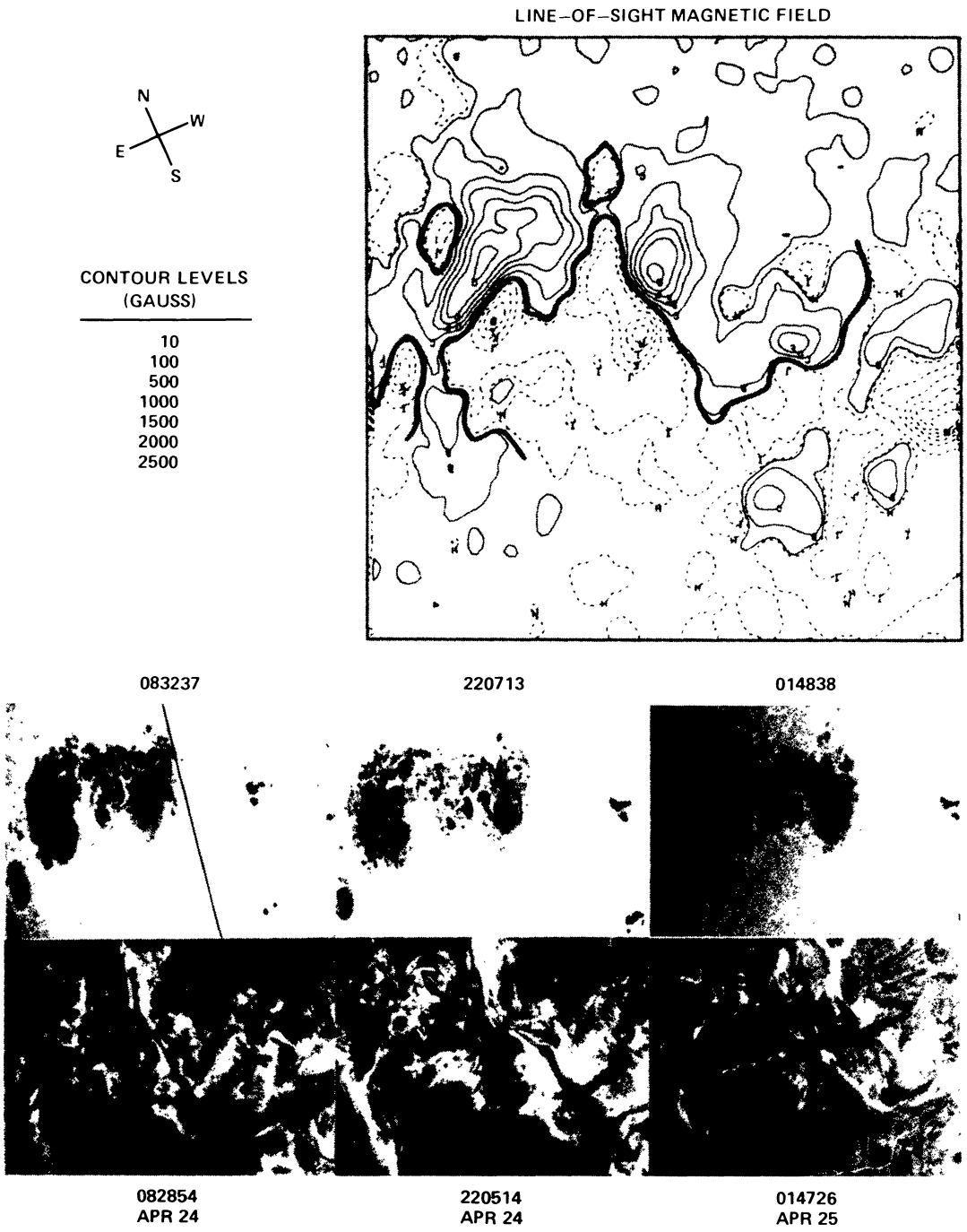

FIG. 1.—Morphology of active region AR 4474 near the time of the great flare on 1984 April 24. In the upper image, a line-of-sight ($B_{\parallel}$) magnetogram taken with the Marshall Space Flight Center's vector magnetograph at 22:11 UT is displayed as contours of positive (*solid curves*) and negative (*dashed curves*) fields over a 5′×5′ field of view. The major magnetic neutral lines are indicated by the heavier solid lines. The "western section" of the neutral line, where the 3B/X13 white-light flare erupted, lies between the opposite polarities at the center of the image. In the lower panels, the active region is seen in white-light and Hα images obtained from the Hida Observatory.

HAGYARD, VENKATAKRISHNAN, AND SMITH (*see* **73**, 160)

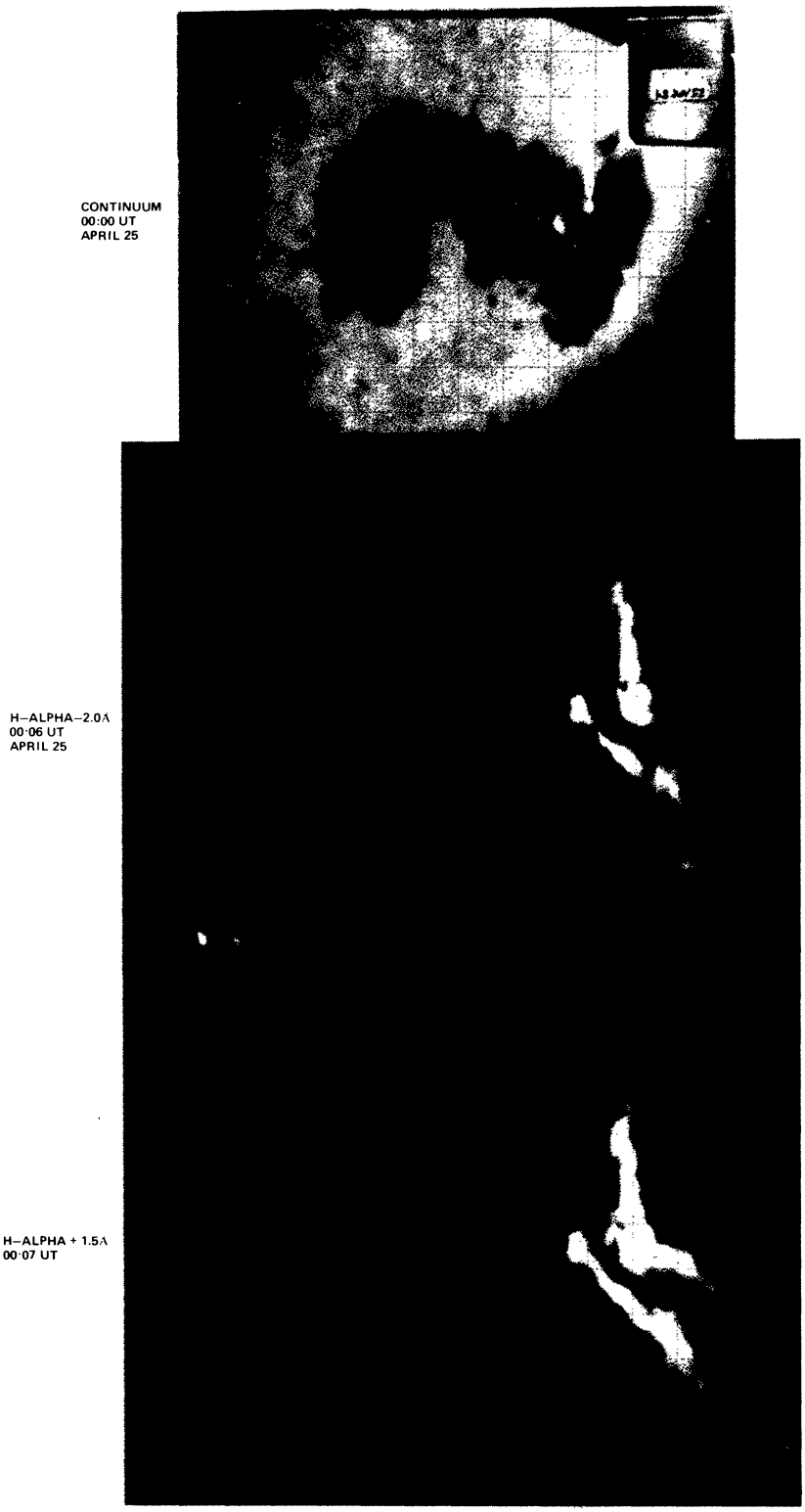

FIG. 2.—Development of the great flare of 1984 April 24. These images show how the flare ribbons bracket the western portion of the magnetic neutral line shown in Fig. 1. These images were obtained at the Big Bear Solar Observatory.

HAGYARD, VENKATAKRISHNAN, AND SMITH (*see* **73**, 160)

1990ApJS...73..159H

FLARE RIBBONS 00:07 UT (APRIL 25)

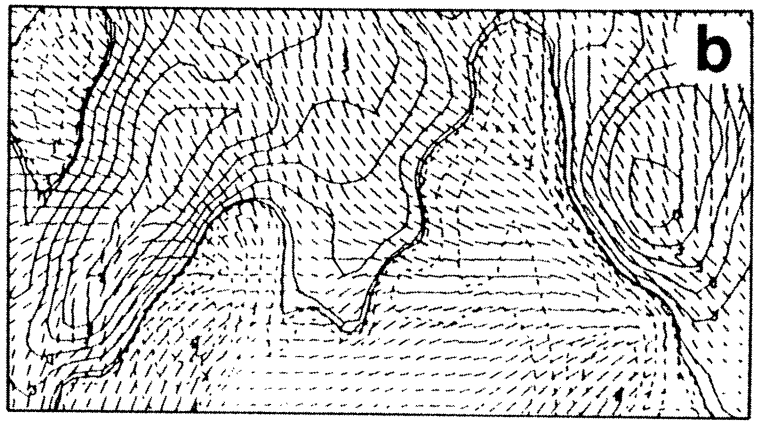

VECTOR MAGNETOGRAM 22:11 UT (APRIL 24)

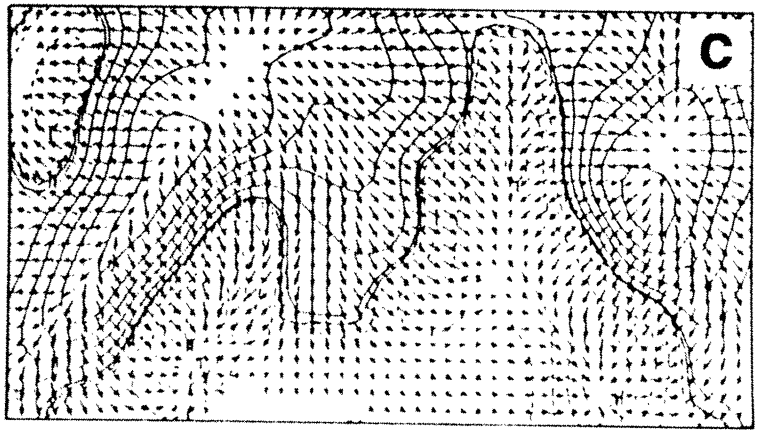

VECTOR POTENTIAL FIELD 22:11 UT

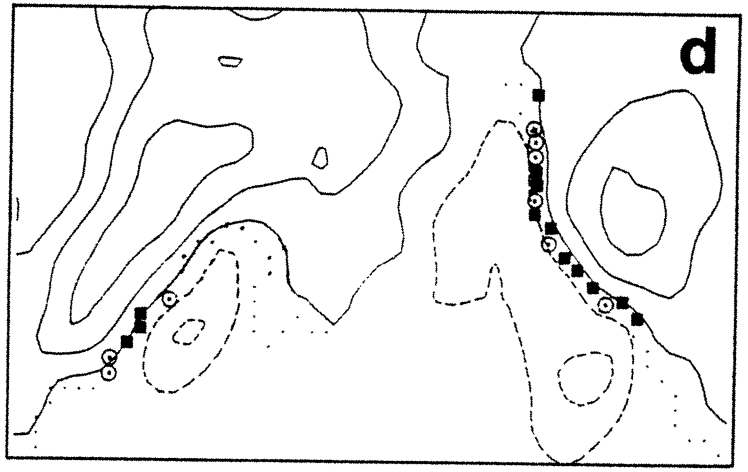

MAP OF MAGNETIC SHEAR 22:36 UT

FIG. 3.—Nonpotential fields in the region of the great flare of 1984 April 24. The flare ribbons shown in (*a*) (from the Big Bear image seen in Fig. 2) bracket the magnetic neutral line seen in the vector magnetogram of (*b*); the magnetogram was obtained at 22:11 UT, 105 minutes prior to the onset of the flare. In this magnetogram the strength and direction of the transverse component (B_T) of the observed field are indicated by the length and orientation of the line segments which are superposed on the line-of-sight field. In (*c*), the transverse component of the potential field is displayed in the same format. From a comparison of (*b*) and (*c*) we recognize that the observed field along the neutral line in the flaring area is highly nonpotential or "sheared." In (*d*), a map of this magnetic shear is shown along the neutral line. Locations of high magnetic shear on the neutral line of the vector magnetogram obtained closest to the time of the flare (at 22:36 UT) are indicated by the open circles and solid squares. The meaning of these symbols is given in the text. Note the extended length of high magnetic shear in the area of the great flare.

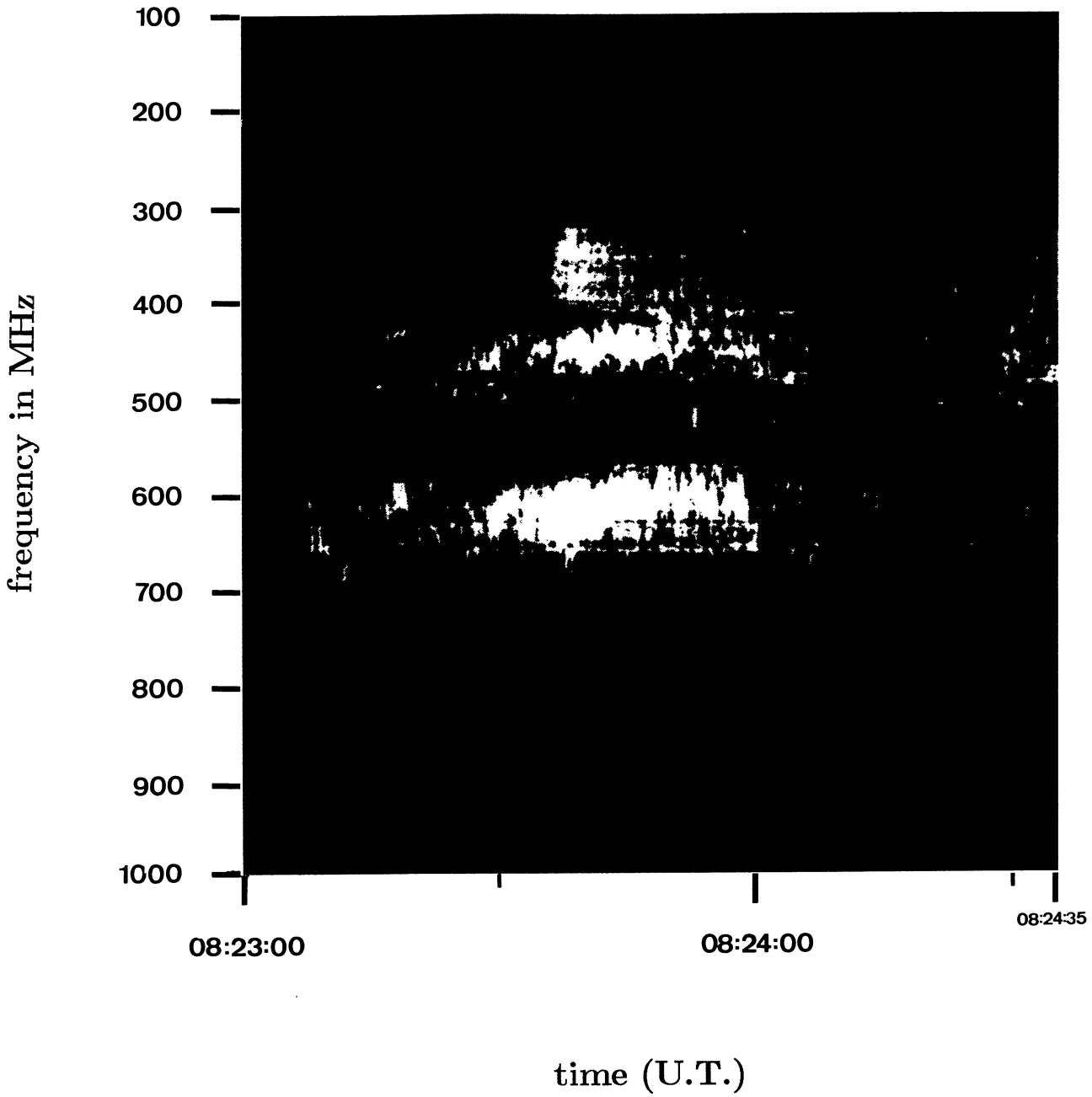

FIG. 4.—(from Benz and Güdel 1987) Analog recording of harmonic structure in a spike event. The radio emission (bright) is shown in the frequency-time plane.

PICK *et al.* (*see* **73**, 168)